Impacts of Extreme Climates on Vegetation in the Middle to High latitudes of Asia

**Yuchen Wei, Miao Yu*, Jiangfeng Wei, Botao Zhou**

*Key Laboratory of Meteorological Disaster, Ministry of Education /Joint International Research Laboratory of Climate and Environment Change (ILCEC) /Collaborative Innovation Center on Forecast and Evaluation of Meteorological Disasters, Nanjing University of Information Science & Technology (NUIST), Nanjing 210044, China*

**Key points**

- Area with maximum/minimum LAI respectively increased/decreased with an increasing/decreasing trend of hot/cold conditions.
- Extreme cold and/or wet conditions inhibited vegetation growth, and extreme hot and/or wet conditions boosted vegetation growth overall.
- Compound hot-and-dry conditions had positive effects on forests, whereas cold and wet conditions were favorable for grasses.

**Abstract:** This study investigated the synchronous responses of vegetation to extreme temperatures and/or precipitation in the middle to high latitudes of Asia using semi-monthly observations of the leaf area index (LAI) from 1982 to 2016. The extreme states of vegetation and climate were specified using standard anomalies of the annual cycle removed variables. The results show that the area with the maximum/minimum LAI increased or decreased in correspondence with global warming. The LAI reached its maximum mostly in spring and autumn, and its minimum in summer. Generally, extreme cold and/or wet conditions inhibited forest and crop growth in the area south of 60°N, particularly from October to November. In contrast, extremely hot and/or dry conditions promoted forest growth, particularly in the central and northern parts of Siberia from August to September. However, in the arid areas of Central Asia and the Mongolian Highlands which are covered mainly by sparse vegetation and grasses, low temperature extremes and/or strong precipitation promoted vegetation growth, while high temperature extremes and/or low precipitation had adverse effects on vegetation growth. The compound extreme climates of hot-and-dry and cold-and-wet were more frequent than the cold-and-dry and hot-and-wet climates. The overall positive response of vegetation was superior to that of the negative response. The results of this study suggest a continuous increase in vegetation density and coverage over the boreal region in the future if the warming trend persists. The consequent climate feedback at regional and global scales should be given more attention.

Plain Language Summary

Extreme climate has significant effects on terrestrial ecosystems and the environment. In recent decades, the middle to high latitudes of Asia have been

experiencing an increasing warming trend and significant changes in extreme climates. To explore the responses of terrestrial vegetation to extreme climate over this area, we utilized the normalized semi-monthly observations of the climate and vegetation density index and leaf area index, with their annual changes removed. Our results show that in general, extreme cold and/or wet climate was unfavorable to forest and crop growth in the area, south of 60°N, particularly at the end or after the growing season. In contrast, an extreme hot and/or dry climate promoted forest growth. However, in the arid areas of Central Asia and the Mongolian Highlands occupied by grasses and sparse vegetation, the responses of vegetation to extreme climates were opposite. This implies that the vegetation density and coverage over the boreal region may continue to increase if the warming trend persists in the future and provide strong feedback on the regional and global climate.

**Keywords:** extreme temperature; extreme precipitation; vegetation responses; middle to high latitudes of Asia.

* Correspondence: yum@nuist.edu.cn; 086-13776503727

## 1. Introduction

Climate change is one of humanity's biggest challenge in the 21st century (Fang et al., 2011). The global 2-meter temperature has increased by 1.53±0.15℃ from 1850–1900 to 2006–2015, and this trend may become more prominent coming decades (IPCC, 2019). Along with the warming trend, most terrestrial areas have been experiencing an increase in warm and hot nights and a decrease in cold days and nights (IPCC, 2012). The frequency and intensity of observed heat-related events have also increased significantly (IPCC, 2012). In future decades, 50–80% of the land area is projected to experience more heat events than the present day (Seneviratne et al., 2016). Although the long-term trend of global drought is still a controversial problem owing to natural variability, potential deficiencies in drought indices, and uncertainty in the quality of precipitation data, changes in the frequency and intensity of drought are evident in some regional areas (Sheffield et al., 2012; Dai, 2013; Trenberth et al., 2014; Mukherjee et al. 2018). A recent global analysis of 4500 meteorological dataset sites found an increase in drought frequency in the east coast of the USA, Amazonia, northeastern Brazil, Patagonia, the Mediterranean region, northeastern China, and most parts of Africa, while a decrease in northern Argentina, Uruguay, and northern Europe was observed (Spinoni et al., 2019). Global warming intensifies the hydrological cycle and affects regional extreme precipitation events (Pall et al., 2007; Berg et al., 2013). During 1981–2010, the number of global record-breaking rainfall events increased significantly by 12% compared to those expected due to multi-decadal climate variability (Lehmann et al., 2015).

Extreme compound events have also triggered increasing attention from the scientific community or climate researchers. The Intergovernmental Panel on Climate Change Sixth Assessment Report (IPCC, 2021) reported that the number of compound dry-hot events worldwide has increased since the 1950s. This increasing trend is projected to continue with a high probability if global warming persists in the future (IPCC, 2021). In particular, compound dry-hot events are likely to occur more frequently in northern Eurasia, Europe, southeastern Australia, the United States, India, and northwestern China (Herrera-Estrada and Sheffield et al., 2017). During 2021, China, Germany, and Bangladesh experienced severe floods; Australia and British Columbia experienced record-breaking wildfires; severe heat waves occurred in Siberia to the Death Valley; and Japan and Texas experienced a destructive typhoon (Yu and Zhai, 2021). Therefore, it is necessary to understand the consequent damage and disasters related to extreme weather and climatic events.

The impacts of extreme climate and weather events on terrestrial ecosystems have triggered interest and attention among researchers worldwide (Islam et al., 2021; Flach et al., 2018). Terrestrial vegetation is a vital component of ecosystems and is a natural bond of energy and masses between the atmosphere and land (Cao and Woodward, 1998). Climate states and variability influence variation in ecosystems (Seddon et al., 2016; Doughty et al., 2015). In general, warm climates promote vegetation growth when energy is the limiting factor for vegetation growth; however, extreme hot climates may inhibit vegetation growth by influencing plant metabolism and cell integrity when water is the limiting factor (Baumbach et al., 2017; Wu et al., 2019; Wen et al., 2019; Karnieli et al., 2010; Hao et al., 2021). The impacts of extreme cold events on ecosystems have also been investigated (Dittma et al., 2006). Studies suggest that extreme cold events during the growing season weaken the water absorption capacity of vegetation, which slows growth. Furthermore, cell dehydration caused by freezing can lead to freezing injury and even the death of plant tissues (Inouye, 2000; Inouye, 2008). Although the number of frost days has decreased in recent decades (IPCC, 2013), this decrease does not always occur during the vegetation growing period; for example, significant increases has been observed in some areas such as Europe. This is because of a longer vegetation growing seasons due to climate warming (Liu et al., 2018). The influence of extreme precipitation on ecosystems mainly depends on the water conditions of the ecosystem during extreme precipitation events (Piao et al., 2019). In arid regions, extreme precipitation increases soil moisture, further increasing ecosystem productivity and carbon accumulation. However, in humid regions, extreme precipitation could impede ecosystem carbon sequestration (Kundzewicz et al., 2014). Many studies have consistently concluded that drought reduces the greenness of vegetation, significantly weakens the carbon sink function of ecosystems, and even transforms terrestrial ecosystem into a carbon source (Knapp and Smith 2001; Jentsch et al., 2011; Zscheischler et al., 2014).

Areas at high latitudes are characterized by short growing seasons due to long cold winters and the persistence of snow (Tuhkanen, 1980). However, since

the Industrial Revolution, the warming trend has been highest in the high latitudes of Eurasia (Hu et al., 2021), with the area experiencing an increase in extreme heat. A warmer climate generally benefits the terrestrial vegetation there because warmer temperatures during the growing season promote photosynthetic activity and enhance terrestrial carbon uptake (IPCC, 2021; Myneni et al., 1997). Using numerical models, some studies have projected that future vegetation coverage will likely expand northward in the high-latitude Northern Hemisphere (Alo and Wang, 2008; Yu et al., 2014; Liu et al., 2020). In Asia, most previous studies concentrated on central Asia, where strong relationships between vegetation greenness and extreme climate with high spatiotemporal heterogeneity have been explored (Jiang et al., 2017; Li et al., 2018; Dubovyk et al., 2016; Luo et al., 2020). However, very few studies have focused on the impacts of extreme climates on terrestrial ecosystems at high latitudes.

Therefore, this study investigated the response of vegetation to extreme temperatures and precipitation over the middle to high latitudes of Asia, using vegetation indices from satellite observations. The remainder of this study is organized as follows. Section 2 describes the study area, data, and methods used. Section 3 focuses on the spatial and temporal distribution of the extreme values of vegetation states. The impacts of extreme temperature and precipitation and compound extremes on vegetation are analyzed in Section 4. The conclusions and discussion are stated in sections 5.

## 1. Study Area, Data and Methods

The studied area is located between 50–160 °E and 30–80 °N, which covers most of the high-latitude area of Asia and extends over a land area of approximately 29,160,490 $km^2$. The vegetation types in this area include broadleaf and needleleaf forests, grasses, shrubs, lichens, and mosses (Fig. 1). The climate of this area is modulated by monsoons, westerlies, and polar weather systems (Liu and Guo, 2005; Yang et al., 2013). For 1986–2016, the annual 2-m air temperature ranged from -4 °C to 30 °C; total precipitation during the growing season of April to November ranged from 200 mm to 1000 mm, and the maximum leaf area index (LAI) was less than 4 (Fig. 2). Most of this area experienced significant increases in the 2-m temperature and LAI during the growing season between 1982 and 2016. Pronounced decreases in precipitation was found in eastern Europe, the Mongolian Plateau, and northeastern China.

Semi-monthly Advanced Very High-Resolution Radiometer (AVHRR) LAI (Zhu et al., 2013) and daily agrometeorological EAR5 datasets (AgERA5) (Hersbach et al., 2020) were used in this study. The LAI dataset was from 1982 to 2016 and had a spatial resolution of 1/12 degrees. The AgERA5 were derived from hourly European Centre for Medium-Range Weather Forecasts (ECMWF) ERA5 data and are presented as input for agriculture and agro-ecological studies. The annual average of the Climate Data Records Land cover (CDR-LC) dataset provided by the Copernicus Climate Change Service (C3S) was used in this study to show the present-day vegetation types, as shown in Fig.1. The AgEAR5 daily 2-m temperature and precipitation were averaged every half month to coincide

with the time frequency of the LAI. The LAI and land cover were aggregated every 0.1° to coincide with the spatial scale of the AgEAR5 dataset. The growing season from April to November was analyzed in this study.

To find the maximum and minimum values of 2 m air temperature, precipitation, and LAI for different years and semi-months, we first removed the 35-year annual cycle and then calculated the standardized anomalies of the variables at each grid to remove the annual changes using Eq. (1) as follows:

$$x_{i,j} = \frac{X_{i,j} - \overline{X}_i}{\mathrm{std}(X_i)} (i = 0, 1, \ldots, 15; j = 1, 2, \ldots, 35) \quad (1)$$

where $x_{i,j}$ is the standardized anomaly of the variable at semi-month i of year j in each grid. $\overline{X}_i$ is the multi-year average of the variable at semi-month I, and std $(X_i)$ is the multi-year standard deviation. $\overline{X}_i$ and std $(X_i)$ were derived from the annual cycle-removed variables. This procedure ensures that the variables are comparable across seasons and years. The maximums (minimums) mentioned below are the maximum (minimum) standardized anomalies throughout the time series. The maximum or minimum values are found in a specific month of a specific year. The $5^{\mathrm{th}}$ and $95^{\mathrm{th}}$ percentiles variables were also analyzed to display the extreme states of climate and LAI at a semi-monthly temporal resolution. The sphere areas with extreme states of variables were calculated at each grid and accumulated to evaluate the geographic scope affected.

1. Extreme States of Vegetation

Before analyzing the impact of extreme 2-m temperature and precipitation, the extreme values of LAI were investigated to explore the spatial and temporal changes in extreme states of vegetation in the study area.

Figure 3a shows that the maximum LAI appeared in most of the area after 2000, and especially in 2011 and 2016. Additionally, in parts of western and southern Siberia, the LAI peaked in 1997. The area with the maximum (minimum) LAI was found to have an (a) increasing (decreasing) trend during 1982–2016 (Fig. 3c and d) with a rate of $2.37\times10^4$ (-0.72) $\mathrm{km}^2$/year, which was caused by the warming trend and corresponds with other studies (Zhu et al, 2016; Chen et al, 2019). The maximum LAI in the area north of 65 °N was mostly observed for June and July, while for the area between 50°N and 60°N, it was mostly observed for April and May or November (Fig. 3e). The LAI in northern Kazakhstan and northeastern China reached its maximum mostly in autumn. However, most of the area reached its minimum LAI in summer, between late July and August. In areas with sparse vegetation and where water is the limiting factor for vegetation growth, such as Kazakhstan and northwestern China, the minimum LAI appeared mostly in spring (Fig. 3f and 3h).

When the LAI peaked, nearly half of the area had a higher than $90^{\mathrm{th}}$ percentile 2-m temperature. This suggests that vegetation growth was significantly promoted when extreme warming occurred in this area. Only some arid and semiarid areas, such as Kazakhstan, indicate that the maximum LAI was accom-

panied by a lower than normal temperature (Fig. 4a). When the LAI reached its minimum, most of the area had a lower than normal temperature, with approximately 40% of the area having a temperature smaller than a 20-percentile. However, in some areas of Kazakhstan, northeast and north China, and central and eastern Siberia, the minimum LAI was accompanied by 2-m temperature higher than the $75^{\text{th}}$ percentile (Fig. 4c). Nearly 17% of the areas had precipitation lower than the $10^{\text{th}}$ percentile with maximum LAI, while about 20% of the areas had precipitation higher than the $90^{\text{th}}$ percentile with minimum LAI (Fig. 4f and 4h). Generally, extreme warm and dry climates favored the growth of vegetation before or after the growing season in the high latitudes of Asia. And the extreme cool with wet climate inhibited the growth of vegetation during the growing season.

1. Impact of Extreme Climate on LAI

4.1 Temperature Extremes

We then focus on the semi-month of a specific year when extreme 2-m temperature or precipitation occurred and explored the synchronous vegetation response. The effects of compound extreme temperatures and precipitation were also explored.

Relatively large areas with a maximum 2-m temperature occurred in early August of 1998 and late May of 2011 in central Siberia, late July of 2011 in the plain south of the Stanovoy Range, and August of 2016 in the northern edge of Siberia and some highlands, such as the southeastern Tibetan Plateau. The area during these three years accounted for 27% of the total area (Fig. 5a–d). The area with the maximum 2-m temperature was found to increase at a rate of $2.47\times10^4$ km$^2$/year ($p < 0.01$), which is consistent with the warming trend from 1982 to 2016. When the maximum 2-m temperature occurred in central Siberia, south-west Siberia, and northeastern China, the percentile of LAI was above the $90^{\text{th}}$ percentile, indicating that extreme high temperatures in these areas would greatly promote vegetation growth. However, in eastern Europe, Kazakhstan, and east Siberia, a less than $10^{\text{th}}$ percentile of LAI was found (Fig. 5e). Figure 5g shows the probability density distribution of the LAI percentiles for different vegetation types. More than half the areas of all vegetation types except cropland and grassland show above normal states. This suggests that extreme warming had a positive effect on vegetation growth in this area, particularly for lichens and mosses.

The minimum 2-m temperature appeared mostly before 2005, accounting for 92% of the total area (Fig. 6a). It appeared mostly at the end of the growing season in October and November, mainly in eastern Kazakhstan, northeastern China, and Siberia (Fig. 6c). Extreme low temperatures occurred mostly within a less than $10^{\text{th}}$ percentile of LAI, suggesting that extreme low temperatures generally limit the growth of vegetation in most parts of the area. However, a greater than $90^{\text{th}}$ percentile of LAI was found in arid and semiarid areas, such as the western parts of Kazakhstan which is covered by sparse vegetation

(Fig. 6e and 6g). Extreme low temperatures generally had a negative effect on vegetation, especially on needle-leaved and broadleaved trees (Fig. 6g).

We further counted the times of the four types when extreme temperatures and extreme LAI occurred simultaneously for each grid (Fig. 7). The extremes were specified if the variables were less than the $5^{\text{th}}$ percentile or greater than the $95^{\text{th}}$ percentile, otherwise they were specified as normal. The four types of extremes were small LAI and cold extremes ($T_S LAI_S$), small LAI and warm extremes ($T_L LAI_S$), large LAI and cold extremes ($T_S LAI_L$), and large LAI and warm extremes ($T_L LAI_L$). As shown in Fig. 7, $T_S LAI_S$ occurred the most frequently, $T_L LAI_L$ the second, and $T_L LAI_S$ and $T_S LAI_L$ were less frequent than the former types. $T_S LAI_S$ occurred mostly between 50°N and 65°N, where broadleaf trees were distributed the most (Fig. 7c and 6g). $T_L LAI_L$ was found mostly in eastern Europe, central Siberia, and some high latitudes around 60°N, where needleleaf trees were distributed. Vegetation in the high latitudes were more sensitive to extreme high temperatures, whereas that in the middle latitudes were more sensitive to extreme low temperatures. $T_L LAI_S$ were concentrated in the northern Mongolian Plateau, and $T_S LAI_L$ seldomly occurred in Kazakhstan.

### 4.2 Precipitation Extremes

Large areas with maximum precipitation occurred in the mountains of eastern Siberia in early October 2016, over an area of 116 million $km^2$. Apart from this, the areas with maximum precipitation had a comparatively scattered distribution (Fig. 8a–d). Extreme precipitation caused a less than $10^{\text{th}}$-percentile LAI to occur in approximately 20% of areas, showing a negative response of vegetation to extreme wetness over this area. However, large areas in Kazakhstan covered by sparse vegetation were found to be greater than the $90^{\text{th}}$ percentile LAI, suggesting a prompting effect of extreme precipitation on vegetation growth in the dry area (Fig. 8e–f). The average percentiles of all vegetation types were less than 50%, indicating that extreme precipitation was unfavorable for all vegetation types. The negative effects were most significant for trees, whereas they were comparatively small for crops, grasses, and sparse vegetation (Fig. 8g).

The overall response of vegetation to extreme dryness was positive in this area, in which the area greater than $90^{\text{th}}$ percentile of LAI was the largest (Fig. 9f). This was likely related to the increase in solar radiation. A negative response was found mainly in the transition zone from desert areas to vegetated areas, such as the central Mongolian Plateau and central China. The positive effects of extreme dry were obvious on mixed trees, lichens, and mosses (Fig. 9g).

Four types of extreme precipitation vs. extreme LAI, that is, extreme wet/drought and large/small LAI ($P_L LAI_L$, $P_L LAI_S$, $P_S LAI_L$, and $P_S LAI_S$), were also counted. Figure 10 shows that $P_L LAI_S$ and $P_S LAI_L$ occurred more frequently than the other two types, suggesting that extreme precipitation generally had a negative effect on vegetation over this area. $P_L LAI_S$ mainly occurred between 50°N and 60°N, particularly in the southern part of central Siberian and northeastern China, where trees occupied the most land area.

$P_S LAI_L$ mainly occurred in the central Siberian Plateau, which is composed mostly of by needle-leaved trees and grasslands. This negative response of vegetation to precipitation was caused by the corresponding positive effect of temperature (Fig. 7) and is likely related to the corresponding change in solar radiation. The frequency of $P_S LAI_S$ was nearly negligible. The frequency of $P_L LAI_L$ was also relatively low. However, it was mainly concentrated in Kazakhstan and the Mongolian Plateau, where sparse vegetation was mostly distributed and showed a positive response to vegetation growth.

1. Compound temperature and precipitation extremes

After exploring the effects of extreme temperatures and precipitation on LAI, we investigated the possible effects of compound extreme temperatures and precipitation. Based on the justification of extreme 2-m temperature and precipitation (Fig. 11), four types of compound extreme climates were identified. The four types of compound extreme climate were dry and cold ($P_S T_S$), wet and hot ($P_L T_L$), dry and hot ($P_S T_L$), and wet and cold ($P_L T_S$). We then counted the time of occurrence for each type in each grid and calculated the corresponding average percentile of LAI for each type. The most frequent compound extreme climate in this area was $P_S T_L$ (Fig. 11d). It was mainly found between 50°N and 60°N in Asia, central Siberia, and central China. In south-central Siberia and central China, the $P_S T_L$ climate generally promoted vegetation growth to an extent (Fig. 11h). The second most frequent compound extreme climate was $P_L T_S$ (Fig. 11a), which mainly appeared in the area south of 60°N, particularly in Kazakhstan and the area between central and eastern China. It generally benefited vegetation growth in the arid and semiarid areas. Although occurring with limited frequency, the compound $P_L T_S$ had a detrimental effect on vegetation at high latitudes (Fig. 11e). Only some dry areas in Kazakhstan and scattered areas with sparse vegetation were shown to have a positive effect. The frequency of $P_S T_S$ and $P_L T_L$ climates were found to be considerably lower than that of the former two types. $P_S T_S$ occurred 2–6 in 35 years in central Siberia (Fig. 11c) and was generally accompanied by the prosperity of vegetation (Fig. 11g).

1. Conclusions and Discussion

This study investigated the impacts of extreme climates on vegetation in the middle to high latitudes of Asia from 1982 to 2016 on a semi-monthly frequency. Standardized anomalies with the annual cycle removed were scrutinized to determine the extremes of climate and vegetation states. The results suggest that the area with the maximum/minimum LAI increased or decreased during 1982–2016, which corresponded with the global warming trend. The LAI reached its maximum mostly in spring and autumn, and minimum in summer.

During these 35 years, the study area experienced both increases and decreases in the frequency of extreme hot and cold. Generally, extreme cold accelerated leaf falls during October and November in northern Kazakhstan, southern Siberia, and northeastern Asia, where forests and croplands occupied the most

land area. Extreme heat promoted vegetation growth, particularly during summer in the northern and central parts of Siberia, and northeastern China, where trees occupied a large proportion of land. However, a negative effect of extreme hot and positive effect of extreme cold was also observed, although much less than in the former two situations. The negative effect of heat was found mostly on grass and sparse vegetation in the northern Mongolian Plateau. A positive effect of cold was found mostly on sparse vegetation in central Kazakhstan. The latter two situations may be related to corresponding precipitation changes in arid areas. The impact of extreme precipitation on vegetation was generally negative, with trees around 50°N and 60°N being harmed the most. The most frequent response of vegetation to extreme dryness was positive, and it occurred mostly on mixed trees in central Siberia, and lichens and mosses in the northernmost edge of Asia. This may be related to the synchronous increase in solar radiation and temperature in the area. The positive effect of extreme wetness was found to be much less than that of the former two conditions, and the negative effect of extreme dryness was found to be the least. Extreme precipitation slightly promoted vegetation growth in the arid areas of Kazakhstan and the Mongolian Plateau but inhibited tree growth in areas between 50°N and 60°N.

The most frequent compound extreme climate of temperature and precipitation was $P_S T_L$, followed by $P_L T_S$. $P_S T_L$ occurred over a vast area that excluded the boreal region, highland area, and desert covered by sparse vegetation. Overall, this condition had positive effects, including promoting the greening of forests and crops. $P_L T_S$ occurred mostly south of 60°N, which covers Kazakhstan, the northern Mongolia Highland, and the area between central and eastern China. Although it seldom occurred in high latitudes, this condition was found to significantly damage boreal vegetation. $P_S T_S$ was observed in central Siberia, and generally has a positive effect on forest growth. $P_L T_L$ was observed as the least frequent condition, and its effect varied with location.

Generally, the results of this study show that extreme cold and/or wet conditions are the most unfavorable conditions for forest growth in the study area. These conditions occurred more frequently from October to November than during the growing season. Dry and/or hot conditions were favorable for boreal forests and croplands, particularly during the growing season and before September. The increase in hot areas corresponded to the significant warming trend observed for this area. This observation may suggest that extreme warmth promotes forest growth. The opposite effects of extremes were found mostly in arid areas, that is, Kazakhstan and the Mongolia Highlands which was primarily occupied by sparse vegetation and grass. This implies the existence of a climate response transition from forest to sparse vegetation in this area. The impact of extreme climate on vegetation depends on the local climate and vegetation types.

Compared with previous studies that focused on small areas particularly arid regions, we investigated the response of vegetation to extreme climate in a relatively large area, the boreal region of Asia, at a semi-monthly frequency. Here, we focused on the synchronous response of vegetation to climate, without

considering the subsequent reactions after the extreme events. Some studies suggest that cold temperatures during the dormancy period may favor vegetation growth in the following year (Lian et al., 2021), and grasses could recover soon after a drought event (Hossain and Li, 2021). The possible vegetation responses after extremes in this area should also be studied in the future.

In this study, the relationships of vegetation with extremes on a semi-monthly frequency correspond with previous research, which focus on the relationship between average vegetation and climate. This implies adaptation of the vegetation in this area. It is projected that this greening trend would continue and expand northward. This has been demonstrated in several numerical studies. However, prosperous vegetation in the northern high latitudes are likely to increase the absorption of solar radiation, further increasing the warming trend. How this affects the local and global climate should also be explored

Acknowledgements

Funding for this study was provided by the National Natural Science Foundation of China (grant numbers 41991285 and 42075115).

Conflict of Interest

The authors declare no conflicts of interest relevant to this study.

Data Availability Statement

The 2m-temperature and precipitation data were obtained from the Copernicus Climate Change Service (https://cds.climate.copernicus.eu/cdsapp#!/dataset/sis-agrometeorological-indicator
Semi-monthly LAI data were obtained from Zhu et al. (http://www.mdpi.com/2072-4292/5/2/927). The land cover dataset is also available from the Copernicus Climate Change Service (https://cds.climate.copernicus.eu/cdsapp%23!/dataset/satellite-land-cover).

References

Alo, C. A., & Wang, G. L. (2008). Potential future changes of the terrestrial ecosystem based on climate projections by eight general circulation models. *Journal of Geophysical Research: Biogeosciences*, **113**(G1). https:/doi.org/10.1029/2007JG000528

Baumbach, L., Siegmund, J. F., Mittermeier, M., & Donner R. V. (2017). Impacts of temperature extremes on European vegetation during the growing season. *Biogeosciences*, **14**(21): 4891–4903. https://doi.org/10.5194/bg-14-4891-2017

Berg, P., Moseley, C., & Haerter, J. O. (2013). Strong increase in convective precipitation in response to higher temperatures. *Nature Geoscience*, **6**(3), 181–185. https://doi.org/10.1038/ngeo1731

Cao, M., & Woodward, F. I. (1998). Dynamic responses of terrestrial ecosystem carbon cycling to global climate change. *Nature*, **393**(6682), 249–252. https://doi.org/10.1038/30460

Chen, J. M., Ju, W. M., Ciais, P., Viovy, N., Liu, R.G., Liu, Y., et al. (2019). Vegetation structural change since 1981 significantly enhanced the terrestrial carbon sink. *Nature Communications*, **10**, 4259. https:/doi.org/10.1038/s41467-019-12257-8

Dai, A. G. (2013). Increasing drought under global warming in observations and models. *Nature Climate Change*, **3**, 52–58. https://doi.org/10.1038/NCLIMATE1811

Dittmar, C., Fricke, W., & Elling, W. (2006). Impact of late frost events on radial growth of common beech (Fagus sylvatica L.) in Southern Germany. *European Journal of Forest Research*, **125**(3), 249–259.https:/doi.org/10.1007/s10342-005-0098-y

Doughty, C. E., Metcalfe, D. B., Girardin, C. A. J., Amezquita, F. F., Cabrera, D. G., Huasco, W. H., et al. (2015). Drought impact on forest carbon dynamics and fluxes in Amazonia. *Nature*, **519**, 78–82. https://doi.org/10.1038/nature14213

Dubovyk, O., Landmann, T., Dietz, A., & Menz, G. (2016). Quantifying the impacts of environmental factors on vegetation dynamics over climatic and management gradients of Central Asia. *Remote of Sensing*, **8**(7), 600. https:/doi.org/10.3390/rs8070600

Fang, J. Y., Zhu, J. Y., Wang, S. P., Yue, C., & Shen, H. H. (2011). Global warming, human-induced carbon emissions, and their uncertainties. *Science China Earth Sciences*, **54**(10), 1458–1468. https://doi.org/10.1007/s11430-011-4292-0

Flach, M., Sippel, S., Gans, F., Bastos, A., Brenning, A., Reichstein, M., et al. (2018). Contrasting biosphere responses to hydrometeorological extremes: revisiting the 2010 western Russian heatwave. *Biogeosciences*, **15**(20), 6067–6085. https://doi.org/10.5194/bg-15-6067-2018

Hao. Y., Hao Z. C., Fu Y. S., Feng, S. F., Zhang, X., Wu, X. Y., et al. (2021). Probabilistic assessments of the impacts of compound dry and hot events on global vegetation during growing seasons. *Environmental Research Letters*, **16**(7), 074055. https://doi.org/10.1088/1748-9326/ac1015

Herrera-Estrada, J. E., & Sheffield, J. (2017). Uncertainties in future projections of summer droughts and heat waves over the contiguous United States. *Journal of Climate*, **30**(16), 6225–6246. https://doi.org/10.1175/JCLI-D-16-0491.1

Hersbach, H., Bell, B., Berrisford, P., Hirahara, S., Horanyi, A., Munoz-Sabater, J., et al. (2020). The ERA5 global reanalysis. *Quarterly Journal of Royal Meteorological Society*, **46**(730), 1999–2049. https:/doi.org/10.1002/qj.3803

Hossain, M. L., & Li, J. F. (2021). NDVI-based vegetation dynamics and its resistance and resilience to different intensities of climatic events. *Global Ecology and Conservation*, **30**, e01768. https:/doi.org/10.1016/j.gecco.2021.e01768

Hu, X. M., MA, J. R., Ying, J., Cai, M., & Kong, Y. Q. (2021). Inferring future warming in the Arctic from the observed global warming trend and

CMIP6 simulations. *Advances in Climate Change Research*, **12**(4), 499–507. https:/doi.org/10.1016/j.accre.2021.04.002

Inouye, D. W. (2000). The ecological and evolutionary significance of frost in the context of climate change. *Ecology Letters*, **3**(5),457–463. https:/doi.org/10.1046/j.1461-0248.2000.00165.x

Inouye, D. W. (2008). Effects of climate change on phenology, frost damage, and floral abundance of montane wildflowers. *Ecology*, **89**(2), 353–362. https:/doi.org/10.1890/06-2128.1

Intergovernmental Panel on Climate Change (IPCC) (2012). Managing the Risks of Extreme Events and Disasters to Advance Climate Change Adaptation. In Seneviratne, S., et al. (Eds.), *Changes in Climate Extremes and Their Impacts on the Natural Physical Environment*. (Chap. 3, pp. 111). Cambridge, UK and New York: Cambridge University Press.

Intergovernmental Panel on Climate Change (IPCC) (2013). Climate Change 2013. In Hartmann, D.L., et al. (Eds.), *The Physical Science Basis. Contribution of Working Group I to the Fifth Assessment Report of the Intergovernmental Panel on Climate Change*, (Chap.2, pp.209). Cambridge, UK and New York: Cambridge University Press.

Intergovernmental Panel on Climate Change (IPCC) (2019). Summary for policymakers. In Shukla, P. R., et al. (Eds.), Climate Change and Land: *An IPCC Special Report on Climate Change, Desertification, Land Degradation, Sustainable Land Management, Food Security, and Greenhouse Gas Fluxes in Terrestrial Ecosystems*, (pp.9). Cambridge, UK and New York: Cambridge University Press.

Intergovernmental Panel on Climate Change (IPCC) (2021). Climate Change 2021. In Masson-Delmotte, V., et al. (Eds.), *The Physical Science Basis. Contribution of Working Group I to the Sixth Assessment Report of the Intergovernmental Panel on Climate Change*, (pp.11). Cambridge, UK and New York: Cambridge University Press.

Islam, A. M. T., Islam, H. M. T., Shahid, S., Khatun, M. K., Ali, M. M., Rahman, M.S., et al. (2021). Spatiotemporal nexus between vegetation change and extreme climatic indices and their possible causes of change. *Journal of Environmental Management*, **289**, 112505–112518. https://doi.org/10.1016/j.jenvman.2021.112505

Jentsch, A., Kreyling, J., Elmer, M., Gellesch, E., Glaser, B., Grant, K., et al. (2011). Climate extremes initiate ecosystem-regulating functions while maintaining productivity. *Journal of Ecology*, **99**(3), 689–702. https:/doi.org/10.1111/j.1365-2745.2011.01817.x

Jiang, L. L., Jiapaer, G., Bao, A. M., Guo, H., & Ndayisaba, F. (2017). Vegetation dynamics and responses to climate change and human activities in Central Asia. *Science of Total Environment*, **599**,967−980.

https:/doi.org/10.1016/j.scitotenv.2017.05.012

Karnieli, A., Agam, N., Pinker, R. T., Anderson, M., Imhoff, M. L., Gutman, G. G., et al. (2010). Use of NDVI and Land Surface Temperature for Drought Assessment: Merits and Limitations. *Journal of Climate*, **23**(3), 618–633. https://doi.org/10.1175/2009JCLI2900.1

Knapp, A. K., & Smith, M. D. (2001). Variation among biomes in temporal dynamics of aboveground primary production. Science, 291(5503), 481–484. https:/doi.org/ 10.1126/science.291.5503.481

Kundzewicz, Z.W., Kanae, S., Seneviratne, S. I., Handmer, J., Nicholls, N., Peduzzi, P., et al. (2014). Flood risk and climate change: Global and regional perspectives. Hydrological Sciences Journal, 59(1), 1–28. https:/doi.org/10.1080/02626667.2013.857411

Lehmann, J., Coumou, D., & Frieler, K. (2015). Increased record-breaking precipitation events under global warming. *Climate Change*, **132**(4), 501–515. https://doi.org/10.1007/s10584-015-1466-3

Li, C. L., Wang, J., Hu, R. C., Yin, S., Bao, Y. H., & Ayal, D.Y. (2018). Relationship between vegetation change and extreme climate indices on the Inner Mongolia Plateau, China, from 1982 to 2013. *Ecological Indicators*, **89**, 101−109. https:/doi.org/10.1016/j.ecolind.2018.01.066

Lian, X., Piao, S. L., Chen, A. P., Wang, K., Li, X. Y., Buermann, W., et al. (2021). Seasonal biological carryover dominates northern vegetation growth. Nature Communications. **12**(1), 983. https:/doi.org/10.1038/s41467-021-21223-2

Liu, Q., Piao, S. L., Janssens, I. A., Fu, Y. S., Peng, S. S., & Lian, X., et al. (2018). Extension of the growing season increases vegetation exposure to frost. *Nature Communications*, **9**, 426. https:/doi.org/10.1038/s41467-017-02690-y

Liu, Y., & Guo, Y. (2005). Impact of Pressure System Anomaly over Mid-High Latitude on the Interdecadal Change of East Asia Summer Monsoon. *Plateau Meteorology*, **24**(02), 129–135.

Liu, W. G., Wang, G. L., Yu, M., Chen, H. S., Jiang, Y. L., & Yang, M. J., et al. (2020). Projecting the Future Vegetation-Climate System over East Asia and its RCP-Dependence. *Climate Dynamics*, **55**(9-10), 2725–2742. https:/doi.org/10.1007/s00382-020-05411-2

Luo, M., Sa, C. L., Meng, F. H., Duan, Y. C., Liu, T., & Bao, Y. H. (2020). Assessing extreme climatic changes on a monthly scale and their implications for vegetation in Central Asia. *Journal of Cleaner Production*, 271, 122396. https:/doi.org/10.1016/j.jclepro.2020.122396

Mukherjee, S. A., Mishra, A., & Trenberth, K.E. (2018). Climate change and drought: A perspective on drought indices. *Current Climate Change Reports*, **4**(2), 145–163. https://doi.org/10.1007/s40641-018-0098-x

Myneni, R. B., Keeling, C. D., Tucker, C. J., Asrar, G. & Nemani, R. R. (1997). Increased plant growth in the northern high latitudes from 1981 to 1991. *Nature*, 386, 698–702. https:/doi.org/10.1016/10.1038/386698a0

Pall, P., Allen, M. R., & Stone, D. A. (2007). Testing the Clausius-Clapeyron constraint on changes in extreme precipitation under CO2 warming. *Climate Dynamics*, **28**(4), 351–363. https://doi.org/10.1007/s00382-006-0180-2

Piao, S. L., Wang, X. H., Park, T., Chen, C., Lian, X., He, Y., et al. (2020). Characteristics, drivers and feedbacks of global greening. *Nature Reviews Earth & Environment*, **1**(1), 14–27 https:/doi.org/10.1038/s43017-019-0001-x

Piao, S. L., Zhang, X. P., Chen, A. P., Liu, Q., Lian, X., Wang, X., et al. (2019). The impacts of climate extremes on the terrestrial carbon cycle: A review. *Science China Earth Sciences*, **62**(10), 1551–1563. https:/doi.org/10.1007/s11430-018-9363-5

Seddon, A. M. R., Macias-Fauria, M., Long, P. R., Benz, D., & Willis, K. J. (2016), Sensitivity of global terrestrial ecosystems to climate variability. *Nature*, **531**, 229–232. https://doi.org/10.1038/nature16986

Seneviratne, S. I., Donat, M. G., Pitman, A. J., Knutti, R., & Wilby, R. L. (2016). Allowable $CO_2$ emissions based on regional and impact-related climate targets. *Nature*, **529**, 477–483. https:/doi.org/10.1038/nature16542

Sheffield, J., Wood, E. F., & M.L. Roderick. (2012). Little change in global drought over the past 60 years. *Nature*, **491**(7424), 435–438. https://doi.org/10.1038/nature11575

Spinoni, J., Barbosa, P., De Jager, A., McCormick, N., Naumann, G., Vogt, J. V., et al. (2019). A new global database of meteorological drought events from 1951 to 2016. *Journal of Hydrology: Regional Studies*, **22**, 100593. https://doi.org/10.1016/j.ejrh.2019.100593

Trenberth, K. E., Dai, A. G., van der Schrier, G., Jones, P. D., Barichivich, J., Briffa, K. R., et al. (2014). Global warming and changes in drought. *Nature Climate Change*, **4**(1), 17–22. https://doi.org/10.1038/NCLIMATE2067

Tuhkanen, S. (1980). Climatic parameters and indices in plant geography. *Acta Phytogeographica Suecica* ,**67**, 1—105.

Wen, Y. Y., Liu, X. P., Xin, Q. C., Wu, J., Xu, X. C., & Pei, F. S., et al. (2019). Cumulative Effects of Climatic Factors on Terrestrial Vegetation Growth. *Journal of Geophysical Research: Biogeosciences*, **124**(4), 798–806. https://doi.org/10.1029/2018JG004751

Wu, X. C., Guo, W. C., Liu, H. Y., Li, X. Y., Peng, C. H., & Allen, C. D., et al. (2019). Exposuresto temperature beyond threshold disproportionately reduce vegetation growth in the northern hemisphere. *National Science Review*, **6**(04), 786–795. https://doi.org/10.1093/nsr/nwy158

Yang, S. Y., Wu, B. Y., Zhang, R. H., & Zhou, S. W. (2013). Propagation of Low-Frequency Oscillation over Eurasian Mid–High Latitude in Winter and Its Association with the Eurasian Teleconnection Pattern. *Chinese Journal of Atmospheric Sciences*, **38**(1), 121–132. https:/doi.org/10.3878/j.issn.1006-9895.2013.12181

Yu, M., Wang, G. L., Parr, D., & Ahmed, K. H. (2014). Future changes of the terrestrial ecosystem based on a dynamic vegetation model driven with RCP8.5 climate projections from 19 GCMs. *Climatic Change*, **127**(2), 257–271. https:/doi.org/10.1007/s10584-014-1249-2

Yu. R., & Zhai, P. (2021). Advances in scientific understanding on compound extreme events. *Transactions of Atmospheric Sciences*, **44**(05), 645–649. https://doi.org/10.13878/j.cnki.dqkxxb.20210824006

Zhu, Z. C., Bi, J., Pan, Y. Z., Ganguly, S., Anav, A., Xu, L., et al. (2013). Global Data Sets of Vegetation Leaf Area Index (LAI)3g and Fraction of Photosynthetically Active Radiation (FPAR)3g Derived from Global Inventory Modeling and Mapping Studies (GIMMS) Normalized Difference Vegetation Index (NDVI3g) for the Period 1981 to 2011. *Remote Sensing*, **5**(2), 927–948. https:/doi.org/10.3390/rs5020927

Zhu, Z. C., Piao, S. L., Myneni, R. B., Huang, M. T., Zeng, Z. Z., Canadell, J. G., et al. (2016). Greening of the Earth and its drivers. *Nature Climate Change*, **6**(8), 791–795. https:/doi.org/10.1038/NCLIMATE3004

Zscheischler, J., Mahecha, M. D., von Buttlar, J., Harmeling, S., Jung, M., Rammig, A., et al. (2014). A few extreme events dominate global interannual variability in gross primary production. *Environmental Research Letters*, **9**(3), 035001. https:/doi.org/10.1088/1748-9326/9/3/035001

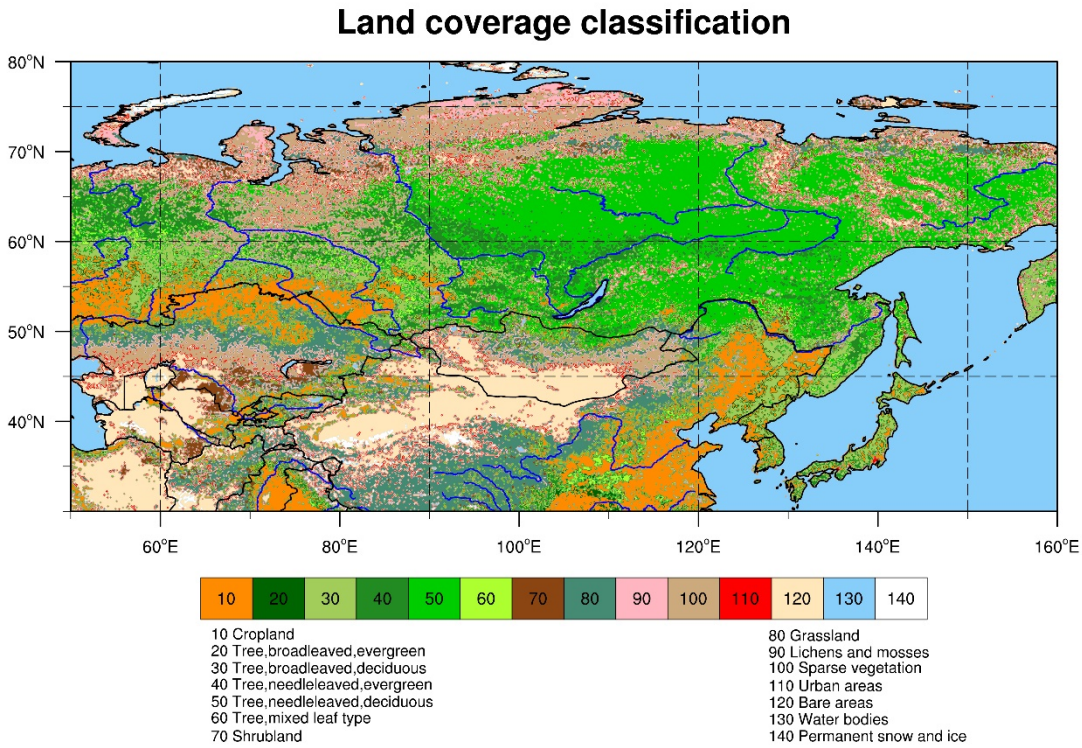


**Fig. 1** Distribution of vegetation types from 1992 to 2016. The reclassification is based on the United Nations Food and Agriculture Organization's (UN FAO) Land Cover Classification System (LCCS).

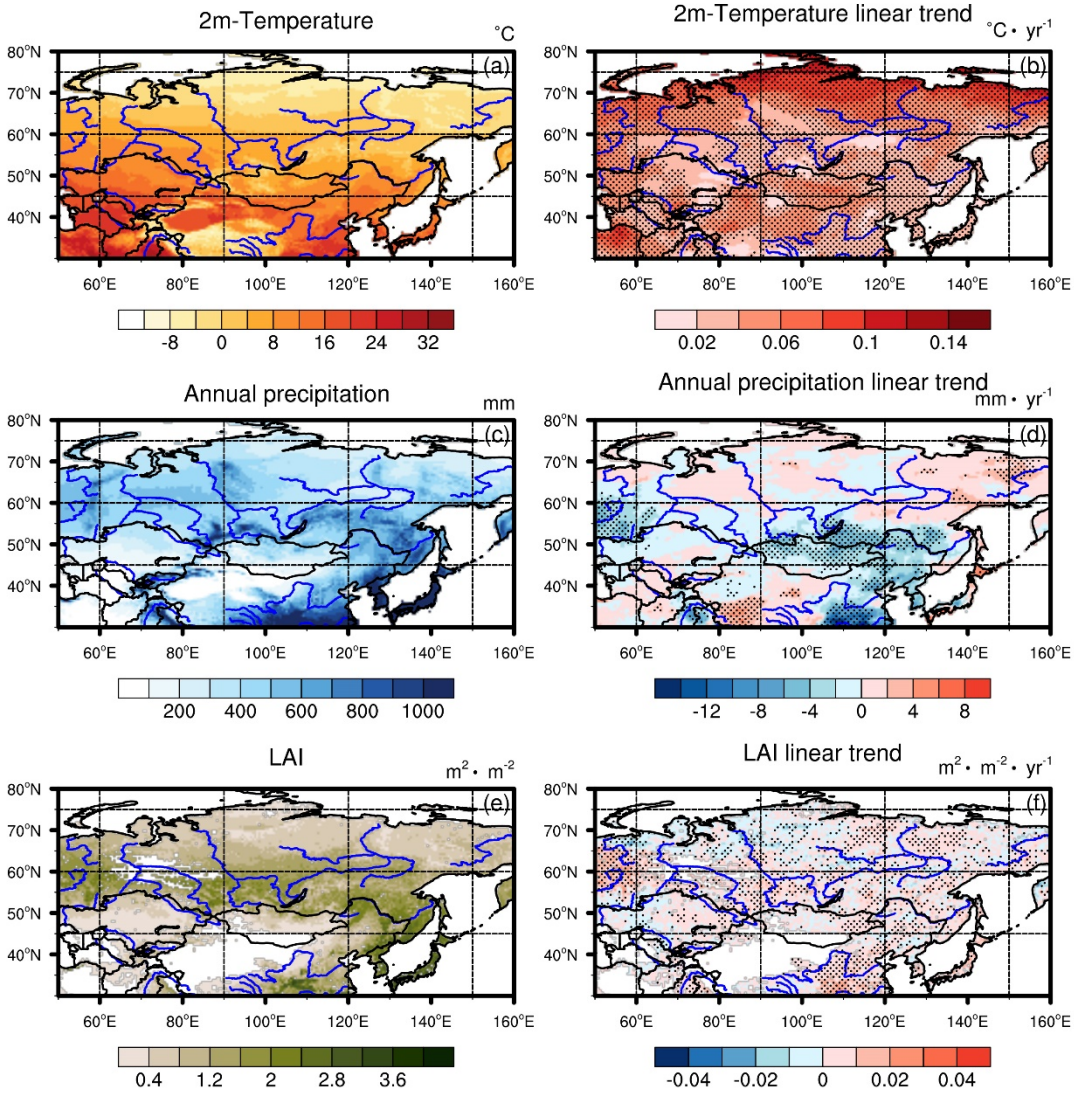


**Fig. 2** Averages of 2-m temperature (a), total precipitation (b), and LAI (c) from April to November 1982-2016, and their linear trends (b, d, f). The stippling means the trends are statistically significant at 5% level of the two-tailed Student's t test.

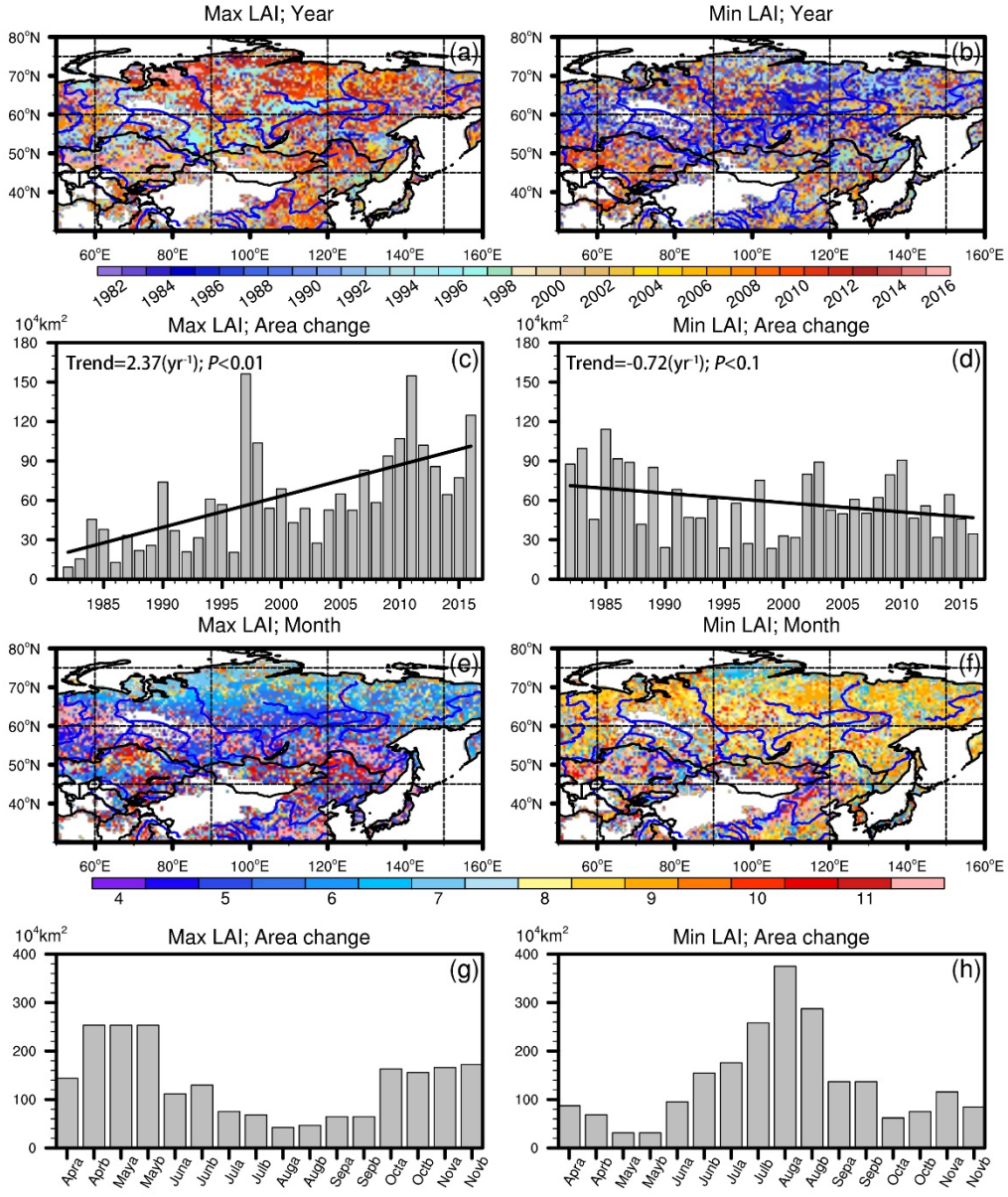


**Fig. 3** Year (a, b) and month (e, f) when the maximum and minimum of LAI occurs. The histograms in c, d, g, and h show the area (unit in $10^4$ km$^2$) that the maximums and minimums occur in different years and semi-months. Lines in c and d are the linear trend of area changes calculated by least-squares regression. The missing values are masked.

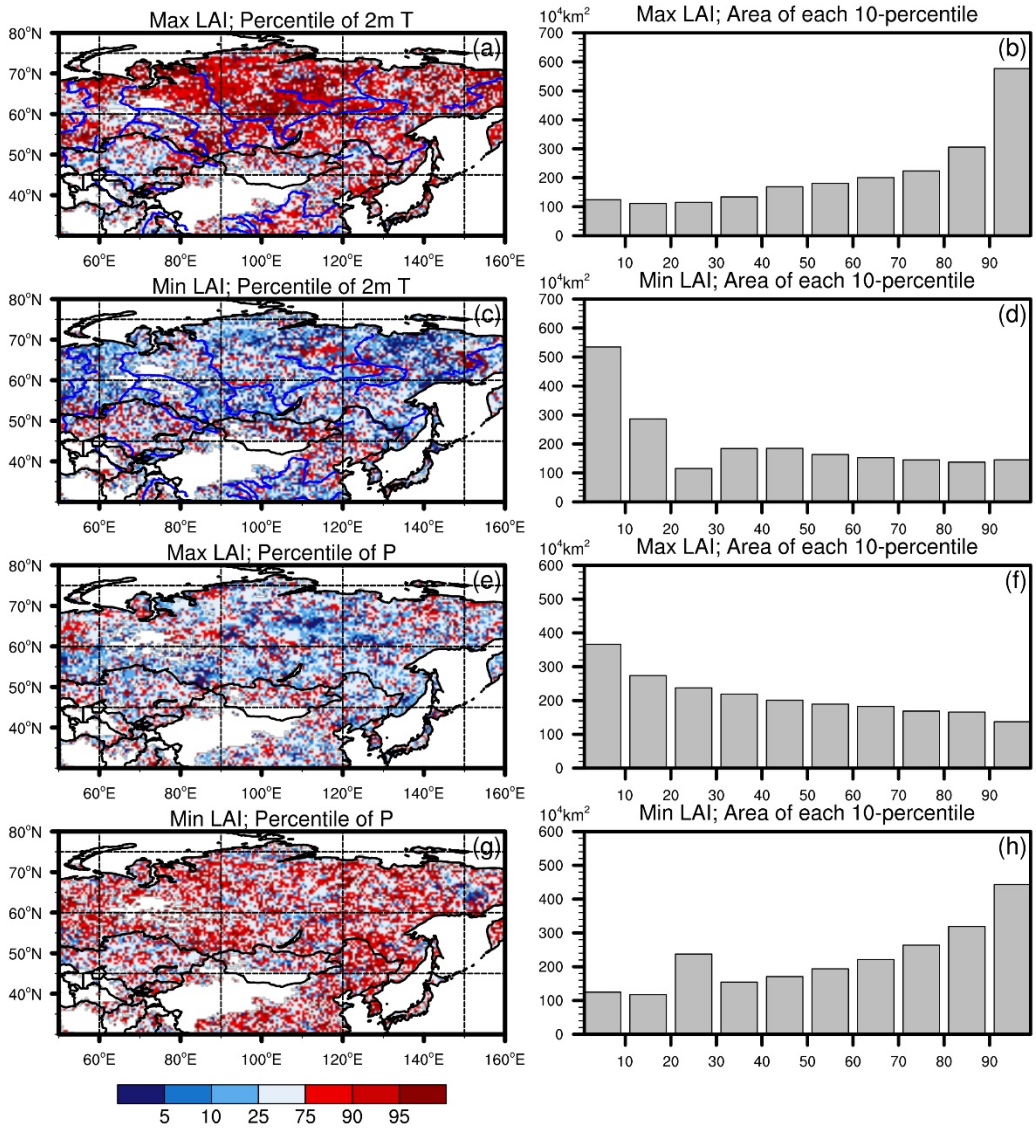


**Fig. 4** Percentiles of 2-m air temperature (a, c) and precipitation (e, g) when maxima (a, e) and minima (c, g) LAI occur. The histograms in b, d, f, and h show the corresponding percentile distributions of the accumulated area (unit in $10^4$ km$^2$).

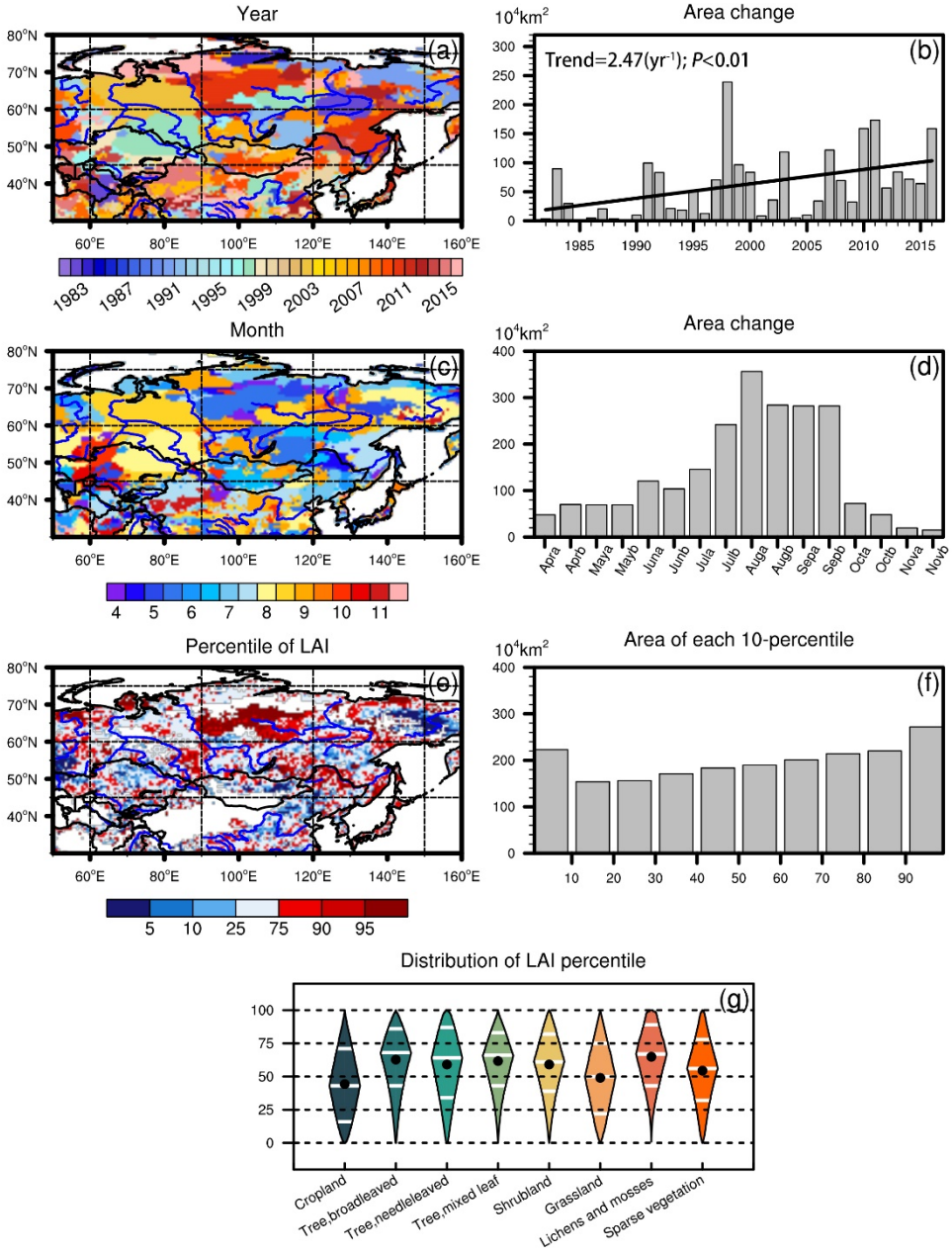


**Fig. 5** Year (a), semi-month (c), and the percentiles of LAI (e) when the maximum 2-m temperature occurs, and the corresponding accumulated areas (unit in $10^4$ km$^2$. b, d, and f). The box plot (g) shows the percentile of LAI for different vegetation types, with the white lines showing the percentile of 25$^{\text{th}}$, 50$^{\text{th}}$, and 75$^{\text{th}}$, and the dots showing the averages. The line in b is the linear

trend calculated by the least-squares regression.

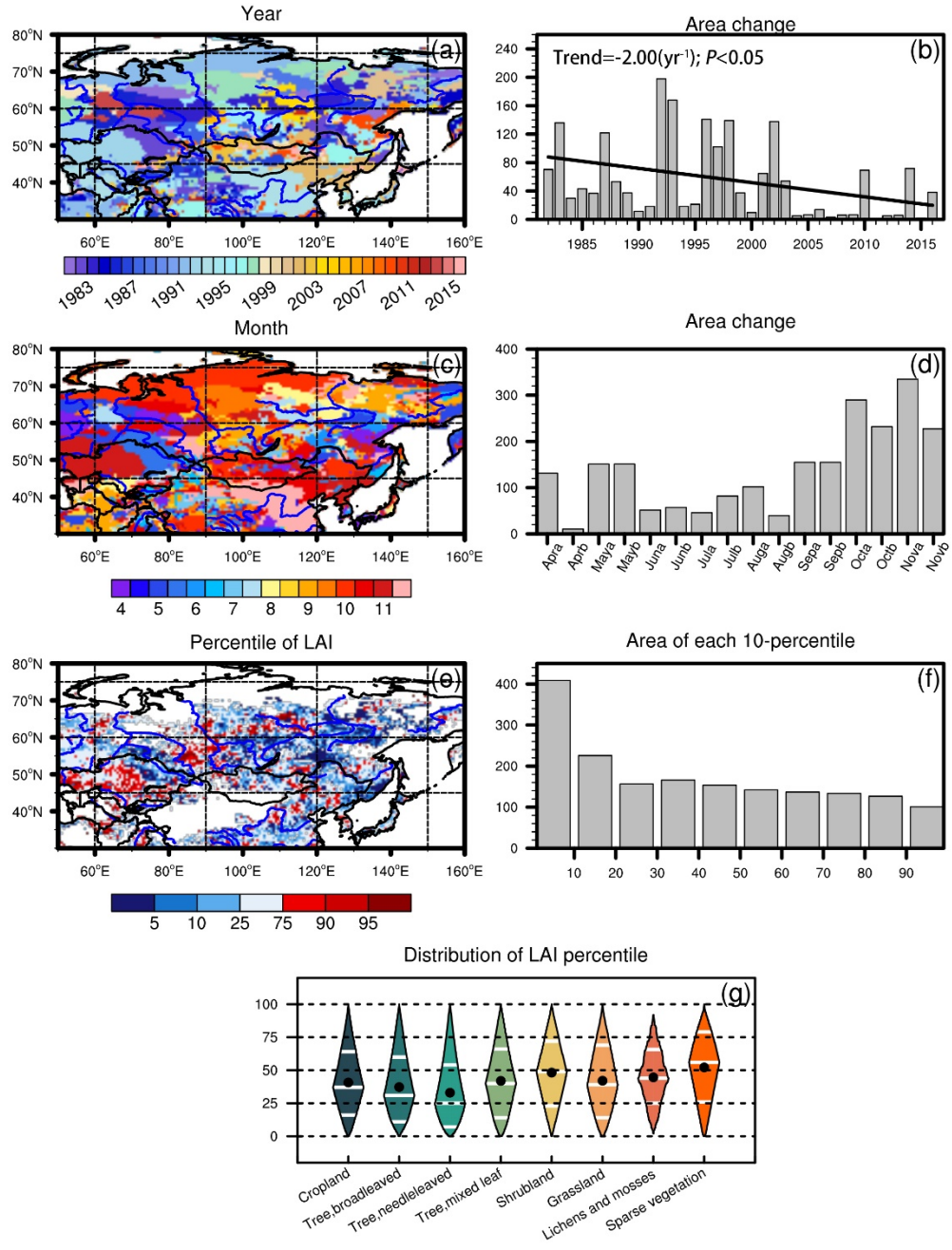


**Fig. 6** Same as Fig. 5 but for the LAI when the minimum 2-m temperature occur.

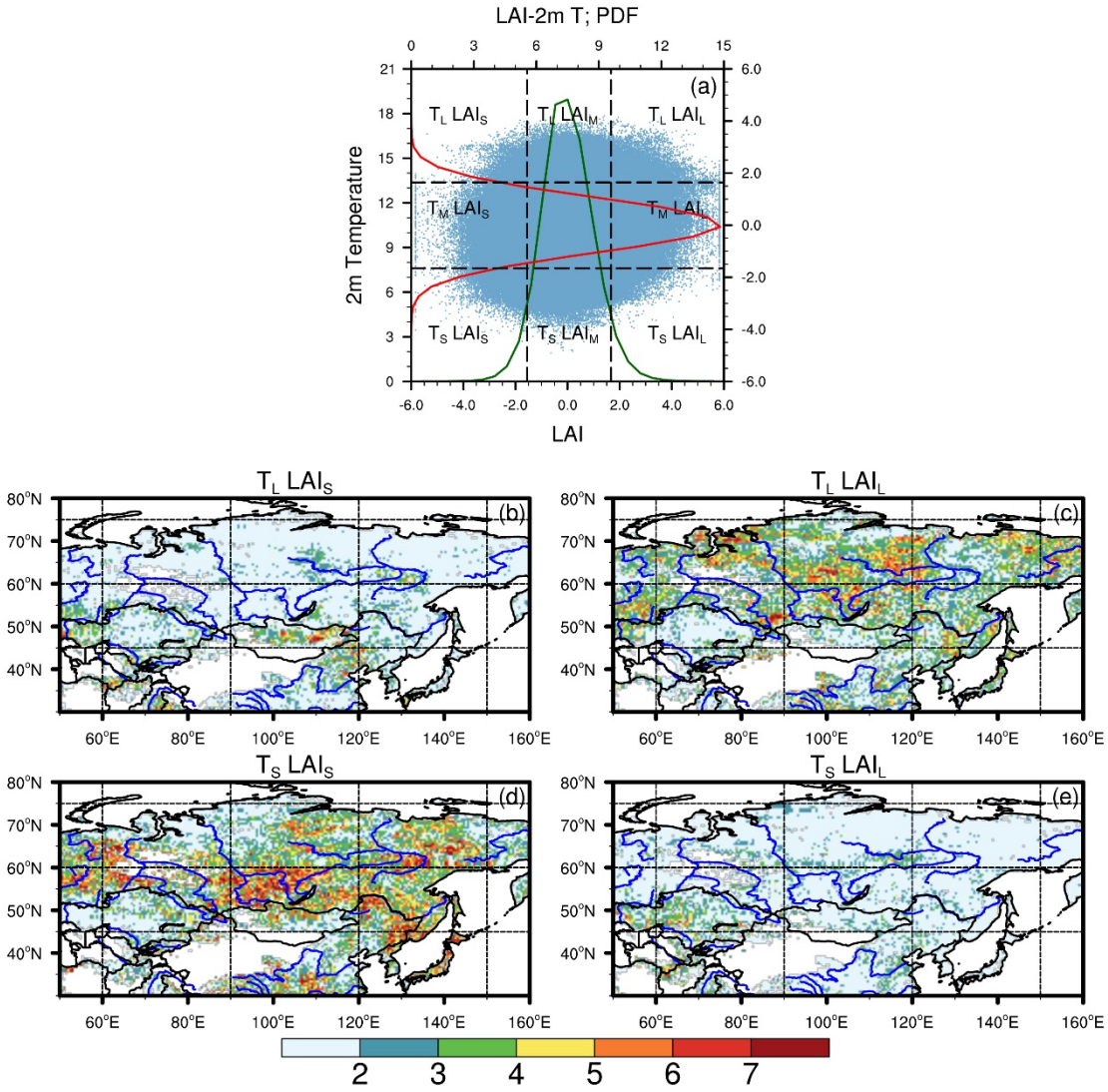


**Fig. 7** (a)Scatter plot of 2-m temperature and LAI with their probability distributions overlaid (lines). The black dashed lines mark the of $5^{th}$ and $95^{th}$ percentiles. The subscripts "L," "S" and "M" represent values of the variables larger than $95^{th}$ percentile, between $5^{th}$ and $95^{th}$ percentile, and smaller than $5^{th}$ percentile, and between $5^{th}$ and $95^{th}$ percentile, respectively. (b-e) Frequencies of the 4-compound extreme LAI-vs-extreme temperature situations (b–e).

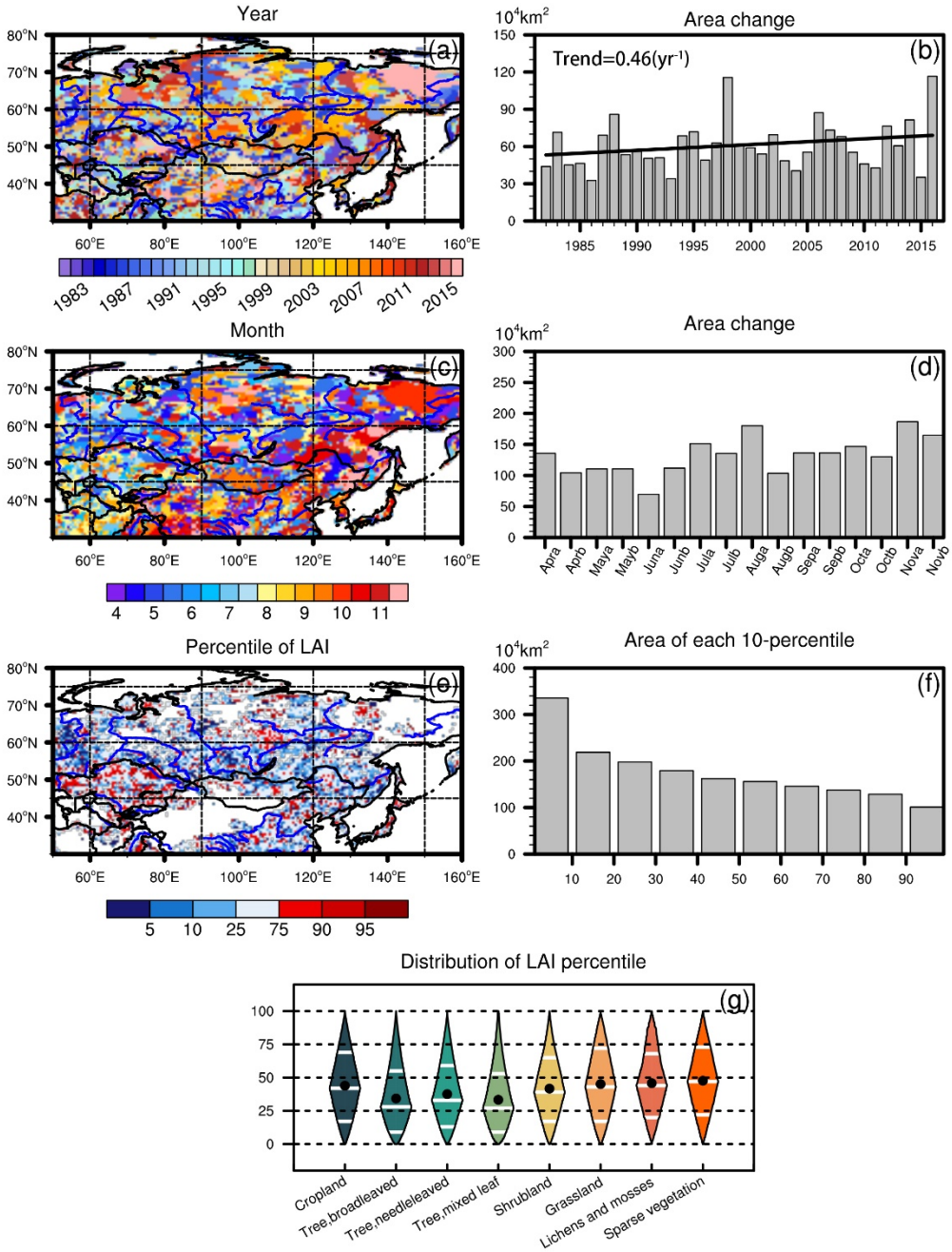


**Fig. 8** Same as Fig. 5 but for the LAI when the maximum precipitation occurs.

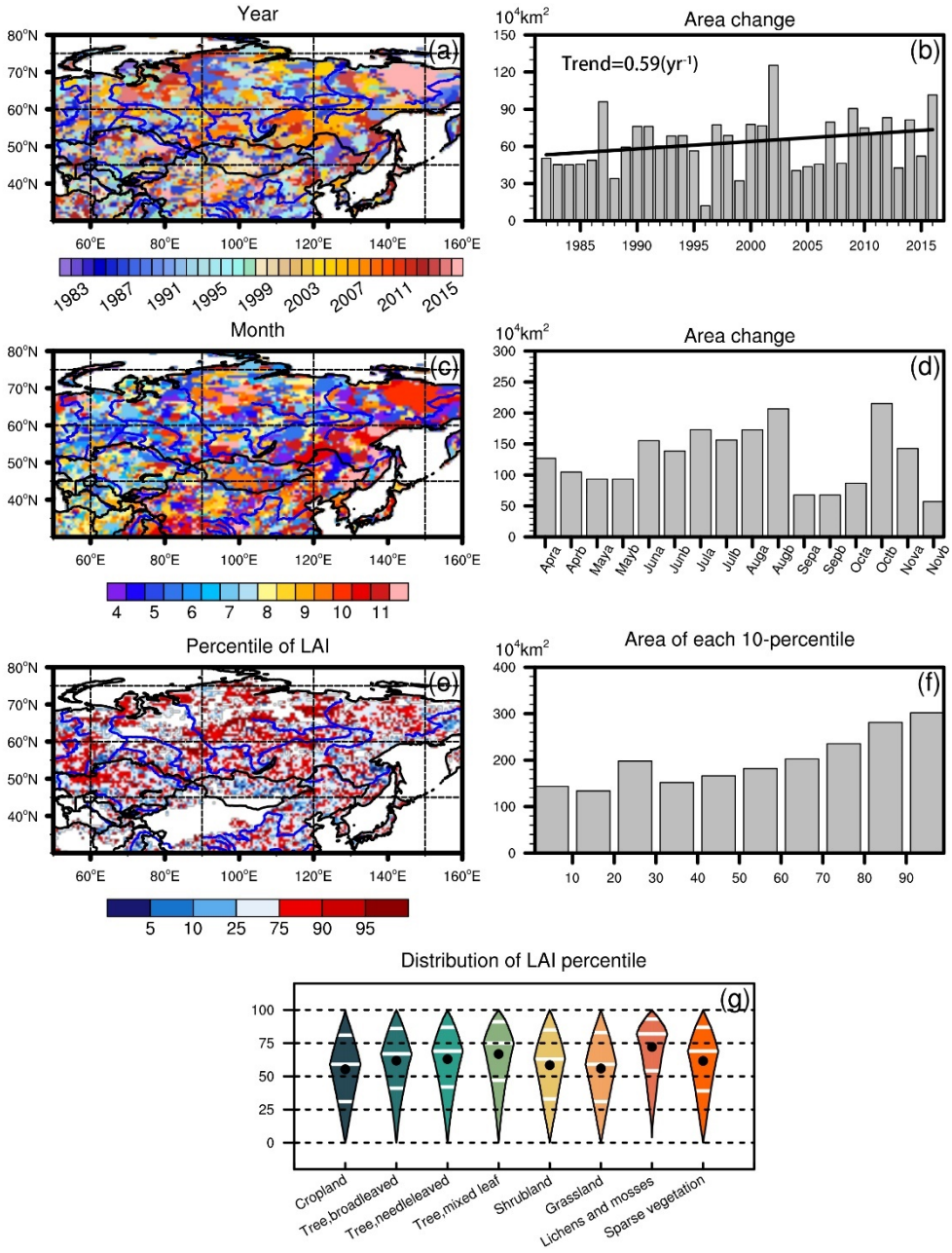


**Fig. 9** Same as Fig. 5 but for the LAI when the minimum precipitation occurs.

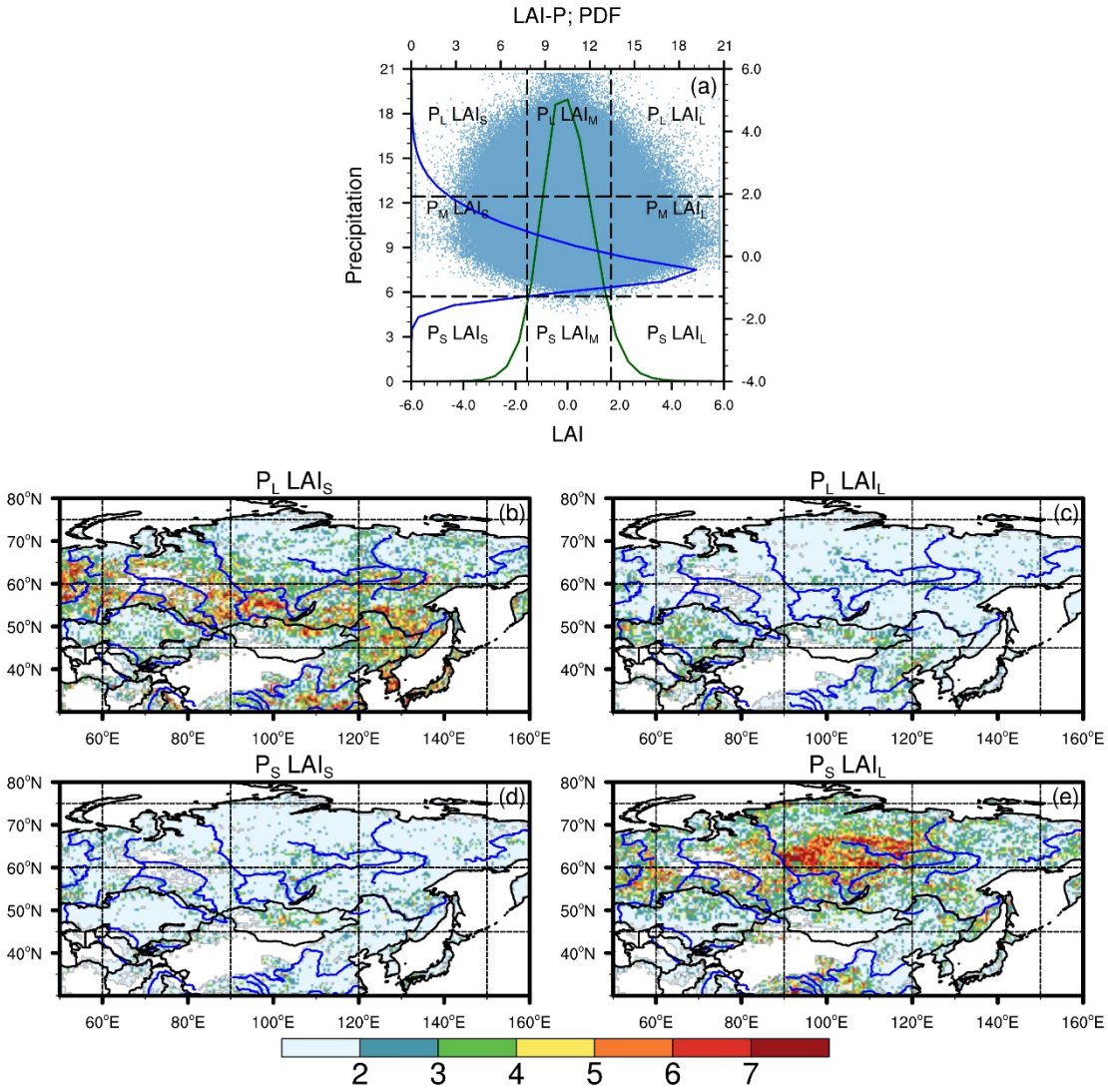


**Fig. 10** Same as Fig. 7 but for the precipitation-LAI relationship.

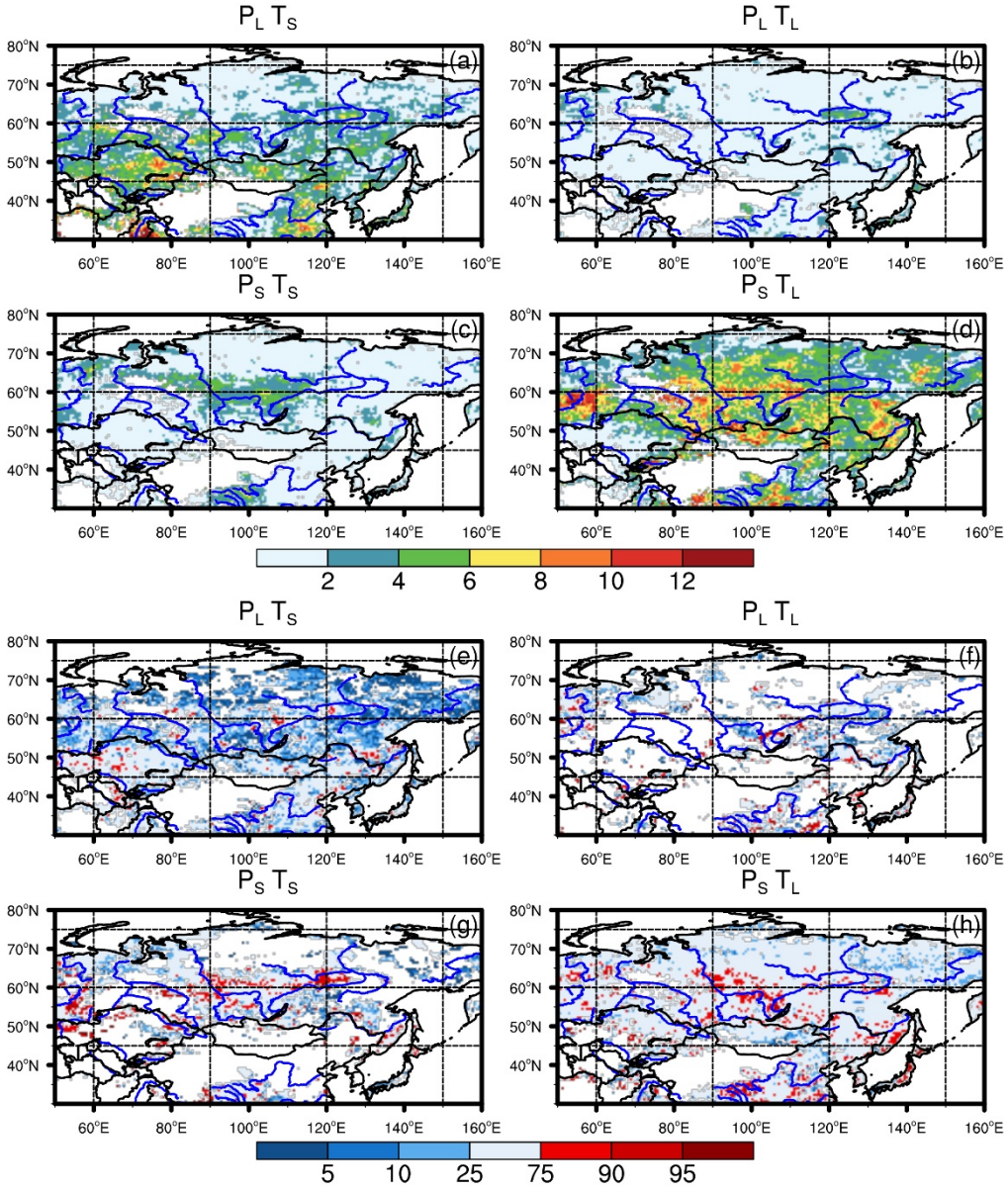


**Fig. 11** Frequencies of the four types of compound extreme precipitation and temperature climates (a–d), and the corresponding average percentiles of the LAI for the four types of compound extreme climates (e–h).